Turbulent Mixing of an Axisymmetric Jet of Partially Dissociated Nitrogen with Ambient Air

T. J. O'Connor,* E. H. Comfort,† and L. A. Cass‡
Avco Corporation, Wilmington, Mass.

Radial and axial variations of fluid properties, i.e., velocity, enthalpy, concentration, and density, in free, compressible, turbulent, jets of partially dissociated nitrogen (T_j = 5800°K) issuing into ambient air were determined experimentally. Investigations were confined to the near flowfield of the jets produced by an electric-arc plasma generator since 90% of the change in jet centerline properties occurred within 45 nozzle radii. Radial property variations were well represented by the Gaussian curve usually found in studies of cold turbulent jets. Integration of the observed radial profiles at several axial stations demonstrated that jet fluid, energy, and momentum fluxes remained constant (±10%) at each station. Centerline jet fluid concentration decayed most rapidly with axial distance; centerline enthalpy, in turn, decayed more rapidly than velocity. Experimental data obtained in these studies were in excellent agreement with a recent integral analysis.

Nomenclature

C_p = specific heat at constant pressure
h = enthalpy
H = $(h_s-h_a)/(h_{s_\mathbb{C}}-h_a)$
$H_\mathbb{C}$ = $(h_{s_\mathbb{C}}-h_0)/(h_j-h_a)$
K = turbulent exchange parameter for velocity
Le = Lewis number
$\dot{m}$ = mass flow rate
M = Mach number
$\mathfrak{M}$ = molecular weight
P = pressure
Pr = Prandtl number
q = general property
r = radial coordinate
Sc = Schmidt number
T = temperature
u = axial velocity
U = $u/u_\mathbb{C}$
$U_\mathbb{C}$ = $u_\mathbb{C}/u_j$
v = transverse velocity
x = axial coordinate
X = x/r_j
y = mass fraction of initial jet fluid
Y = $(y - y_a)/(y_\mathbb{C} - y_a)$
$Y_{\mathbb{C}'}$ = $(y_\mathbb{C} - y_a)/(y_j - y_a)$
z = transverse coordinate
γ = ratio of specific heats
ϵ = turbulent exchange coefficient
μ = viscosity
ρ = density
ϕ = oxygen-to-nitrogen atom ratio
χ = mole fraction

Subscripts

a = ambient conditions
$\mathbb{C}$ = centerline conditions
e = exit conditions
f = with a gas sample flowing through probe
g = gas
h = enthalpy
nf = without gas sample flowing through probe
s = stagnation conditions
t = turbulent
u = velocity
y = mass fraction
0 = base condition for enthalpy computation
j = initial jet conditions
δ = denotes position within jet at which property is one-half of centerline property

Presented as Preprint 65-823 at the AIAA Aerothermochemistry of Turbulent Flows Conference, San Diego, Calif., December 13-15, 1965; submitted January 4, 1965; revision received May 27, 1966. This research was supported by the Advanced Research Projects Agency, Ballistic Missile Defense Systems Branch, and was monitored by the Dynamics Branch, U. S. Naval Research Laboratory under Contract Nonr 3307(00) (X).

* Senior Scientist, Space Systems Division, Research and Technology Laboratories.

† Senior Scientist, Space Systems Division, Research and Technology Laboratories. Member AIAA.

‡ Senior Staff Scientist, Space Systems Division, Research and Technology Laboratories. Member AIAA.

Introduction

RECENT attempts to predict property variations within high enthalpy compressible free jets have suffered from a lack of experimental data with which analyses can be compared. Although it had been assumed that high-enthalpy gas streams would exhibit turbulent mixing characteristics of cold jets that have been subjected to extensive study, there had been no experimental evidence to support this contention.

Although turbulent jets have been extensively studied, the great bulk of existing experimental data is for unheated jets. A complete bibliography of jet analyses and experiments was given by Forstall and Shapiro[1] in 1950. Schubauer[2] presented a summary of heated jet experiments, but in no case was the ratio of initial jet stagnation temperature to ambient temperature greater than 5.0. Greater rates of spreading and decay were in general noted for heated jets as compared with cold jets.

The only experimental data on jets at temperatures high enough to produce dissociation and/or ionization which are known to have been reported to date is the work of Grey and others at Princeton. He used probes similar to those used in the present study to investigate an arc-heated jet of argon surrounded by an annular stream of unheated helium. Although extremely high temperatures were produced (maximum temperature of 23,800°R), the Mach number of the flow was extremely low ($M < 0.1$). The decay rates observed were extremely large, being about five times faster than those typically observed[3] for cold jets. It was suggested that the apparently large scale of turbulence might be the cause of the high decay rate. Grey noted that the scale of turbulence was apparently generated within the nozzle, possibly by the arc itself, and could not be controlled by flow parameter variations. In general, the results of studies conducted with heated jets and with jets having compositions that differed from ambient revealed that turbulent mixing of mass and enthalpy was more rapid than momentum transfer.

The submerged turbulent jets under consideration are considered as a class of aerodynamic problems termed "free turbulent flow." When the Reynolds number of the flow, based on jet diameter, is greater than 1000,[5] a zone of turbulent mixing will begin at the point where the emerging jet first comes into contact with the stationary ambient field. A schematic diagram of an axially symmetric free turbulent jet emerging from a nozzle of finite size is shown in Fig. 1. Within the potential core of the jet the inviscid flow solution is applicable and all flow conditions are preserved at their nozzle exit values. However, the turbulent mixing zone, which is initiated at the periphery of the jet, where discontinuities in velocity first exist, spreads to the axis until it comprises the entire flowfield. Downstream of this point the flow is termed "fully developed." In reality, the boundary between the potential core and the fully developed region is not sharply defined, and there is a "transition" region between the two portions of the flowfield.

The boundary-layer equations that are assumed to apply to such flows in the absence of pressure gradients are

$$(\partial/\partial x)(\rho u r) + (\partial/\partial r)(\rho v r) = 0 \tag{1}$$

$$\rho u \left(\frac{\partial u}{\partial x}\right) + \rho v \left(\frac{\partial u}{\partial r}\right) = \left(\frac{1}{r}\right)\frac{\partial}{\partial r}\left(r\mu \frac{\partial u}{\partial r}\right) \tag{2}$$

$$\rho u \frac{\partial y}{\partial x} + \rho v \frac{\partial y}{\partial r} = \frac{1}{r}\frac{\partial}{\partial r}\left(\frac{r\mu}{Sc}\frac{\partial y}{\partial r}\right) \tag{3}$$

$$\rho u \frac{\partial h_s}{\partial x} + \rho v \frac{\partial h_s}{\partial r} = \frac{1}{r}\frac{\partial}{\partial r}\left(\frac{r\mu}{Pr}\frac{\partial h_s}{\partial r}\right) + \frac{1}{r}\frac{\partial}{\partial r}\left(\frac{\mu r}{Pr}\{Pr - 1\}\times \frac{\partial}{\partial r}\frac{u^2}{2}\right) + \frac{1}{r}\frac{\partial}{\partial r}\left(\frac{\mu r}{Pr}\{Le - 1\}\sum_i h_i \frac{\partial y_i}{\partial r}\right) \tag{4}$$

It is obvious that an assumption of Prandtl and Schmidt numbers of unity greatly simplifies the energy and species conservation relationships making these equations formally identical to the momentum equation. The velocity then can be related to enthalpy and jet fluid mass fraction through the Crocco integral.

When all quantities are represented as the sum of a time-averaged and a fluctuating component, substituted into the boundary-layer equations of motion, and the resulting relations are then averaged over time, the fluctuating components disappear except for products of the fluctuations whose mean value is not zero. For axisymmetric compressible flow, the momentum and continuity relations become

$$\rho u \frac{\partial u}{\partial x} + \rho v \frac{\partial u}{\partial r} + \overline{\rho' v'}\frac{\partial u}{\partial r} = -\frac{1}{r}\frac{\partial}{\partial r}(r\overline{\rho u' v'}) \tag{5}$$

$$(\partial/\partial x)(\rho u r) + (\partial/\partial r)(\rho v r + \overline{\rho' v' r}) = 0 \tag{6}$$

These relations are then integrated over the transverse coordinate employing an empirical equation for the radial variations in jet fluid properties. The usual formulation of the property variation in the developed region is taken to be[3,7,8]

$$q'/q_{\mathfrak{L}} = \exp\{-0.6932(r/r_5)^2\} \tag{7}$$

The apparent shear stress ($\rho u'v'$) is usually related to the velocity gradient by the expression

$$-\rho u' v' = \rho\epsilon(\partial u/\partial r) \tag{8}$$

where ϵ is the turbulent exchange coefficient and is equivalent to the kinematic viscosity in laminar flows. The various hypotheses that have been employed to relate the turbulent exchange coefficient with the mean quantities of the flow have been reviewed by Warren.[7] The relation generally applied to free turbulent flows is Prandtl's hypothesis,[2] which results in

$$\epsilon = Kb(u_{max} - u_0) \tag{9}$$

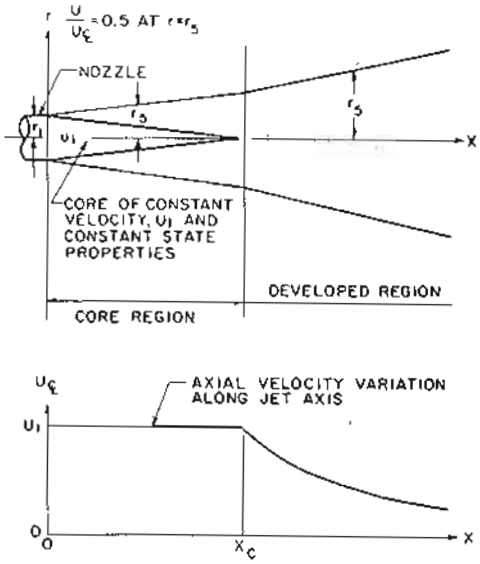

Fig. 1 Schematic diagram showing the coordinate system.

for any cross section of the flow where b is a measure of the jet width and u_0 is the velocity at b. In the fully developed region of the flow the characteristic jet dimension is the jet half-width (r_5), defined as the radial distance at which the local velocity is exactly one-half the centerline velocity. The turbulent exchange coefficient then can be expressed as

$$\epsilon = Kr_5 u_{\mathfrak{L}}/2 \tag{10}$$

In addition, it is evident that, in free turbulent flows, the momentum, energy, and jet fluid (in contrast to ambient fluid) fluxes must remain constant at each plane perpendicular to the jet axis. Therefore at each axial position the following relationships must apply:

$$2\pi \int_0^\infty \rho u^2 r\, dr = \text{const} \tag{11}$$

$$2\pi \int_0^\infty \rho u(h_s - h_a) r dr = \text{const} \tag{12}$$

$$2\pi \int_0^\infty \rho u(y - y_a) r dr = \text{const} \tag{13}$$

Warren[7] performed an integral analysis of jet mixing in which he assumed the parameter K to be constant throughout the flowfield. By comparison of experimental data with his analysis he found that K could be expressed in terms of the initial jet conditions as

$$K = 0.0434\text{–}0.0069\, M_1 \tag{14}$$

Warren's analysis has recently been extended by Donaldson and Grey[8] to the very high temperature jet in which dissociation and large density differences occur. They assumed $Sc_i = 1$ in addition to $Pr_i = 1$. Unlike Warren's analysis, their analysis indicates that K is a function of axial position and can be correlated with the Mach number $M(x, r_5)$.

The objective of the present study was to extend the experimental knowledge concerning turbulent jet mixing to high-enthalpy levels at high subsonic Mach numbers, a realm not previously investigated, and to compare the experimental results with available analyses. The experimental property variations in the radial direction are to be compared with the form of the radial profiles usually assumed in integral analyses of turbulent jet mixing.

Apparatus, Test Conditions, and Procedure

The jet mixing experiments were performed in the high enthalpy exhaust jet produced by a 1.5-Mw electric arc gas

...anode and cathode configuration.

heater.[9] In essence, the arc heater consisted of a cathode assembly, an anode assembly, a plenum chamber and an exit nozzle as shown schematically in Fig. 2. Electric power to the plasma generator was supplied by two Perkin-Elmer 0.5-Mw rectifiers. Gas entered the plasma generator through a series of inlet holes in the wall of the chamber located between the anode and cathode. The gas stream was heated to a high temperature (6000°K) as it flowed through the electric discharge between the anode and cathode and then was exhausted to atmosphere through the arc exit nozzle. A 29-in.-diam baffle plate was located in the nozzle exit plane to simulate a jet issuing from a hole in an infinite wall. Nitrogen (commercial grade) was employed as the working fluid in all experiments in order to obtain the long arc running times required for conducting the investigations.

Arc operating conditions were selected to insure that the high-temperature exhaust jets were turbulent and had high subsonic Mach numbers. During the course of the investigations, three arc operating conditions (Table 1) were employed. Measurements of radial and axial property variations were made at the first operating condition, whereas only centerline property decay was determined for the two remaining points.

Since flow instabilities associated with peculiarities of the electric arc heater would grossly affect the experimental data, considerable effort was expended in investigating the time characteristics[10] of the plasma-generator exhaust jet. High-speed motion pictures (2000–8000 frames/sec) demonstrated that jet flapping instabilities similar to those noticed by Grey and Jacobs[3] in their investigations were essentially eliminated with the arc configuration employed in this study. In addition, measurement of the sound pressure level of the exhaust jet indicated white noise (120 db) over the entire frequency range from 20 to 10,000 cps.

Variations in the free jet velocity, enthalpy, and concentration were determined from measurements made with water cooled enthalpy and pressure probes. The cooled enthalpy probe (0.187-in. o.d.) was similar to that described by Grey.[11] The instrument required the measurement of the inlet and exit cooling water temperature, the exit temperature of a gas sample drawn through a sampling tube (0.042-in. i.d.) located on the probe axis, and coolant water and gas sample flow rates for determination of the local gas stagnation enthalpy. With the exception of gas flow rate, all subsidiary measurements were performed using standard techniques. In drawing the gas sample, care was taken to insure that sonic velocity was obtained at the rear of the probe gas sample line. Hence the gas flow rate remained constant during sampling. Collecting the gas in a known volume and measuring the initial and final pressure and temperature allowed the flow rate to be determined from the equation of state, provided the gas composition was known. Local values of the stagnation pressure within the jet were determined during the course of the enthalpy measurements by placing a calibrated pressure transducer in the sampling line between the probe and the valve, which, when opened, allows a gas sample to be drawn through the probe. A portion of the gas

...characters upstre... members in order to minimize the dist... probe structure on the pressure mea... static pressures were found to be wit... at every position within the jet. Th... occurred at the axial position corresp... potential core.

The probes employed in the jet d... placed in the flowfield by means of ... which could move the instruments i... and axial directions. The various lea... ment of the probes allowed their locatio... determined with an accuracy of 0.01 i... forming the radial surveys at each axi... were taken to insure that each probe m... horizontal plane, which passed throug... mum jet stagnation pressure. A sim... followed in measurement of jet centerlin...

Data Reduction

The basic principle employed in con... obtained with the enthalpy probe to ... thalpy in the jet was an energy balance ... sample and the probe cooling water. T... probe from the heated jet was determine... gas sample through the probe and the... through the sampling tube. Measur... temperature rises, gas and coolant flow ... perature as it left the probe allowed the ... to be determined from

$$h_s = \frac{\dot{m}_{H_2O} C_{p_{H_2O}} \Delta T_f - \Delta T_{gf}}{\dot{m}_g} + C$$

When it is assumed that thermodynam... static pressure of 1 atm prevailed everywhe... the stagnation enthalpy stagnation press... position were sufficient to determine all oth... quantities of interest such as speed of so... ratio, density, temperature, etc., by an it... As a first approximation, the stagnation ... sumed to be the static enthalpy allowing th... and specific heat ratio to be computed from ... tionships. The local freestream Mach n... evaluated from the isentropic flow relationsh...

$$P_s/P = [1 + [(\gamma - 1)/2]M_s^2]^{\gamma/(\gamma-1)}$$

and the local velocity was simply the produ...

Table 1 Summary of 1.5-Mw/arc operat... jet mixing experiments

Operating conditions	1	2
I, amp	990	990
V, v	400	400
r_0, in.	0.375	0.37...
h_0/h_s	33.64	34.5...
h_0, Btu/lb	4460	458...
T_{s0}/T_∞	19.45	19.5...
M_∞	0.782	0.67...
% N_2 dissociated	8.5	9.0

. and the sound speed. A new estimate of static enthalpy s then given by

$$h_2 = h_{t2} - u_1^2/2 \tag{17}$$

tations were continued until successive approximations to static enthalpy satisfied the criterion

$$(h_{i+1} - h_i)/h_{i+1} \leq 0.005 \tag{18}$$

local freestream velocity was taken to be u_{i+1} and state variables were computed from thermochemical equilibrium using the static enthalpy, static pressure, and gas composition as independent variables.

The local composition in the jet was converted from free oxygen concentrations determined by the oxygen analyzer to a mass fraction of initial jet fluid by means of the procedure described below. A recent analysis[14] of rapid quenching of oxygen-nitrogen mixtures from high temperatures in small-diameter tubing has shown that, for initial gas temperatures in the vicinity of 5000°K, the concentration of nitric oxide remained constant at its freestream equilibrium concentration throughout the cooling process. However, at room temperature, chemical kinetic[15] considerations indicated that the nitric oxide would be almost completely converted to nitrogen dioxide (or its dimer) by reaction with oxygen within a short period of time. Considering the stoichiometry of the reactions,

$$2NO + O_2 \rightarrow N_2O_4 \qquad N_2O_4 \overset{K_p}{\rightleftharpoons} 2NO_2$$

the fact that the argon-to-oxygen atom ratio in the sample was identical to that in air, and the fact that, by definition, the sum of the mole fractions is unity, the oxygen-to-nitrogen atom ratio can be expressed as a function of the free oxygen mole fraction in the cold sample (χ_{O_2}) and the nitric oxide mole fraction in the jet (χ_{NO}):

$$\phi = \frac{\chi_{O_2} + \chi_{NO}\mathfrak{M}_c/\mathfrak{M}_A}{1 - 1.0448\chi_{O_2} - (\alpha/2 + 0.0448)\chi_{NO}\mathfrak{M}_c/\mathfrak{M}_A} \tag{19}$$

The degree of N_2O_4 dissociation (α) was defined by means of the equilibrium constant as

$$K_P = [2\alpha^2/(1 - \alpha)]\chi_{NO}P\mathfrak{M}_c/\mathfrak{M}_A \tag{20}$$

where P was the gas pressure in the sample bottle (1 atm) and $\mathfrak{M}_c$ and $\mathfrak{M}_A$ were the molecular weights of the cold gas sample and the gas in the jet, respectively. As a first approximation, the oxygen-to-nitrogen atom ratio was taken as

$$\phi_1 = \chi_{O_2}/(1 - \chi_{O_2}) \tag{21}$$

and the nitric oxide concentration, and hot and cold molecular weights were determined from chemical equilibrium. An iterative procedure was followed until a suitable convergence interval between successive approximations to the atom ratio was obtained. The jet fluid mass fraction was simply

$$y = \frac{\phi - 3.7175}{1 + \phi[(\mathfrak{M}_O/\mathfrak{M}_N) + 0.0224(\mathfrak{M}_A/\mathfrak{M}_N)]} \tag{22}$$

where $\mathfrak{M}_A$, $\mathfrak{M}_O$, and $\mathfrak{M}_N$ were the atomic weights of argon, oxygen, and nitrogen, respectively, with the constants representing nitrogen-to-oxygen and argon-to-nitrogen atom ratios for air.

Table 2 Momentum, energy, and jet fluid fluxes are operating condition 1

x, in.	$2\pi\int_0^\infty \rho u^2 r dr$, lbm-ft/sec²	$2\pi\int_0^\infty \rho u(h_s - h_a) r dr$, Btu/sec	$2\pi\int_0^\infty \rho u(y - y_a) r dr$, lb/sec
4.0	159	163	4.83×10^{-3}
6.0	147	158	4.76×10^{-3}
8.0	137	144	5.59×10^{-3}
10.0	140	157	5.60×10^{-3}

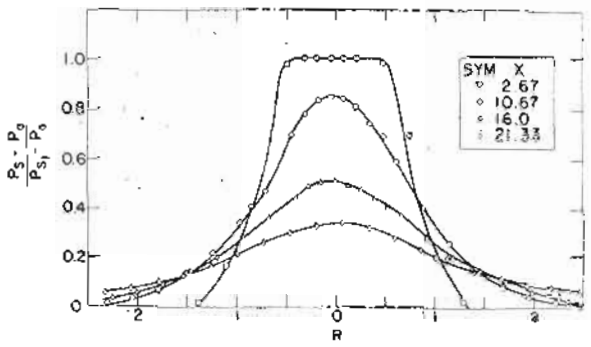

Fig. 3 Stagnation pressure distribution-radial-operating condition 1.

The computation of enthalpy, velocity and mass fraction described above was performed simultaneously by a digital computer program. A more complete description of data reduction procedures can be found in Ref. 10.

Experimental Results

Although enthalpy measurements were made only in the fully developed region of the jet, the existence of a core in the usual sense (Fig. 1) was demonstrated by the stagnation pressure profiles shown in Fig. 3. Radial distributions of jet velocity, enthalpy and jet fluid mass fraction are presented in Figs. 4-6 for the primary operating condition (Table 1) at several axial positions. The radial property profiles were integrated numerically to obtain the momentum, energy, and jet fluid fluxes at each axial station (Table 2). The initial decrease and subsequent increase of momentum flux with axial distance is qualitatively similar to that found by Snedecker and Donaldson[16] for cold jets. They attribute this behavior to pressure gradients set up by the entrained flow on surrounding obstacles including the baffle plate in the exit plane. The increase noted far downstream may have been caused by the exhaust fan located in the wall opposite the jet exit. The energy flux shows a similar behavior. The apparent increase in jet fluid flow rate with

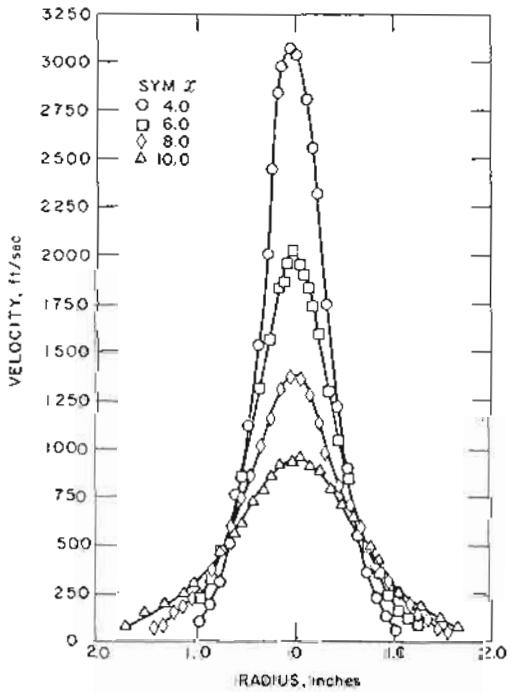

Fig. 4 Velocity distribution-radial-operating condition 1.

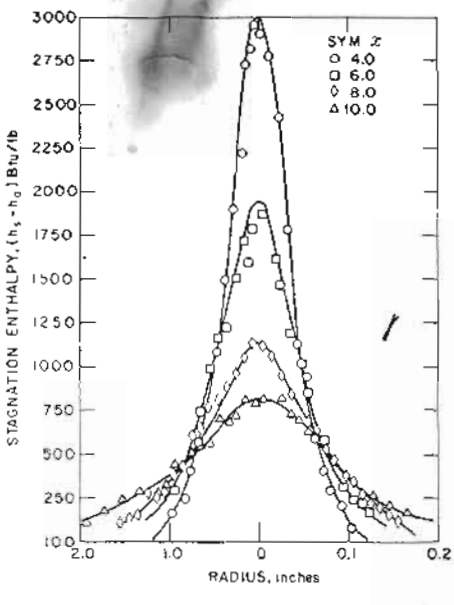

Fig. 5 Stagnation enthalpy distribution-radial-operating condition 1.

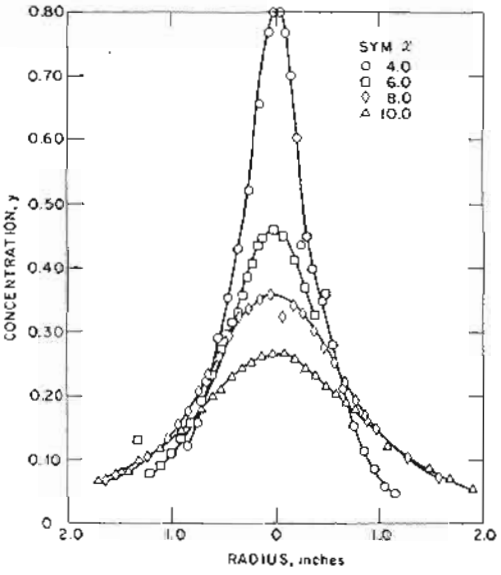

Fig. 6 Jet fluid concentration distribution-radialoperating condition 1.

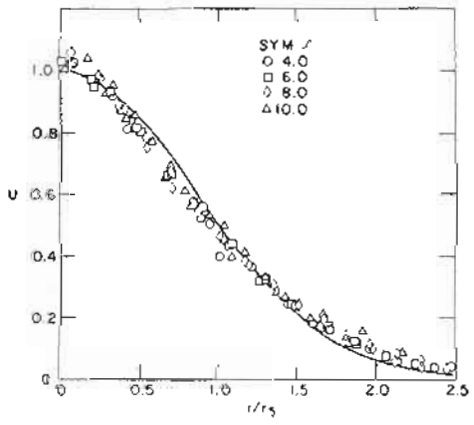

Fig. 7 Radial curve fit-velocity.

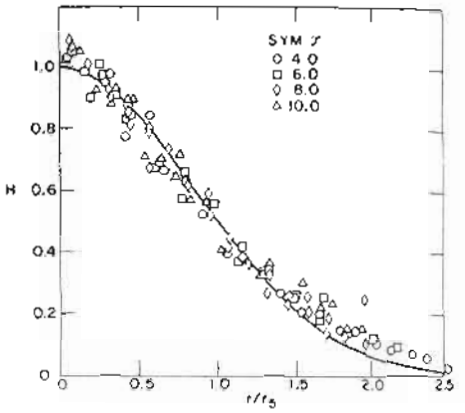

Fig. 8 Radial curve fit-stagnation enthalpy.

downstream distance may be due to the nitrogen enrichment of the ambient fluid, which was caused by operating the nitrogen arc for long periods of time. Thus, downstream where entrained fluid composes a greater proportion of total jet fluid, the assumption that the ambient fluid is standard air may cause increasingly large errors. Nevertheless, momentum, energy, and jet fluid fluxes were found to remain constant to within ±10%. Each radial property was normalized and compared to the form of the property variation[3,7,8] usually assumed to hold in integral analyses of turbulent jet mixing [see Fig. (7)].

Normalized property variations are presented in Figs. 7 a Although the least-squares Gaussian error curve gave somewhat faulty agreement at the outer edge of the flowfield the agreement was good in generally and the the similarity of the profiles was obvious. A number of data points near the centerline were found to be larger than unity because the value of the centerline property resulting from a least-mean square curve fit to all the data was slightly less than the experimental centerline value.

The jet half-width (r_5), which denotes the radial spread of the jet, was used to characterize the turbulent mixing (Fig. 10). The half-width boundaries of the jet were not linear functions of axial distance as is the case for incompressible jets. The curvature of the experimental boundaries resulted from a combination of compressibility effects and the fact that at 4.0 in. from the arc exit nozzle the flow was in transition between potential flow in the core and fully developed flow further downstream. The concentration half-width increased most rapidly with axial distance; the enthalpy half-width was, in turn, larger than the velocity half-width at each axial station. This order of mixing was in agreement with the results of Jacobs.[17]

Reichardt[2] suggested that the Prandtl number in for turbulent flows could be evaluated from experimental data

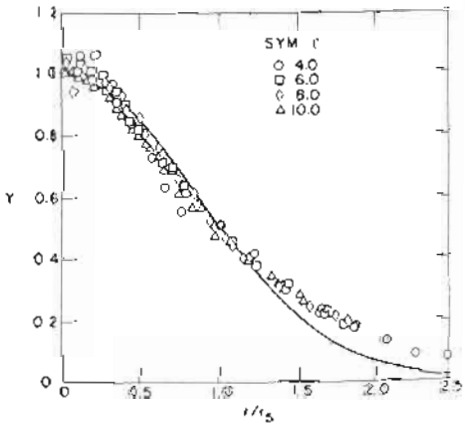

Fig. 9 Radial curve fit-concentration.

Table 3 Turbulent Prandtl, Schmidt, and Lewis numbers operating condition 1

x, in.	Pr_t	Sc_t	Le_t
4	0.93	0.74	1.25
6	0.79	0.57	1.39
8	0.64	0.50	1.32
10	0.64	0.51	1.25

the relationship

$$(h_s - h_a)/(h_{s_\xi} - h_a) = (u/u_\xi)^{Pr_t} \tag{23}$$

ation of the property profile [Eq. (7)] results in a ship between the property half-widths and the turbu- Prandtl number

$$Pr_t = (r_{5u}/r_{.5h})^2 \tag{24}$$

the enthalpy ratio is replaced by the concentration the exponent in Eq. (23) becomes the turbulent Schmidt ber and an expression similar to that for the Prandtl ber is obtained. On this basis turbulent Prandtl, dt and Lewis numbers were evaluated at each axial (Table 3). These tabulated values may be taken dication of the errors inherent in analyses of turbulent which assume equal rates of momentum energy, and transfer in free turbulent flows.[7,8]

Axial surveys of velocity, enthalpy, and concentration performed for all three arc operating conditions. The centerline was taken to be the locus of points at which a maximum impact pressure was observed. The observed centerline decay with axial distance of jet velocity, stagnation alpy, and jet fluid mass fraction for operating condition presented in Figs. 11–13. Over the range of the initial conditions considered, there was very little effect of initial Mach number and/or enthalpy ratio on the centerline For each arc operating condition, enthalpy decayed rapidly than did velocity. Initially, the jet fluid mass tion decreased in a manner similar to enthalpy, but far stream concentration decayed at a rate similar to ve- These variations in the behavior of centerline con- tration were attributed to the nitrogen enrichment of the ent fluid as discussed earlier.

The velocity decay was compared (Fig. 11) with the in- pressible relationship of Hinze and Van der Hegge [ref.], the compressible analysis of Kleinstein,[19] and the nt analysis of Donaldson and Gray.[8] The highly heated pressible jets considered in the present study has shorter lengths and more rapid decay than predicted by the mpressible formulation. Although the work of Klein- [19] was found to be valid for slightly compressible jets, d not predict the behavior noticed in the present study, aps because of the linearized asymptotic nature of the tion. Agreement between the experimental data and compressible turbulent mixing analysis of Donaldson[8] was ellent.

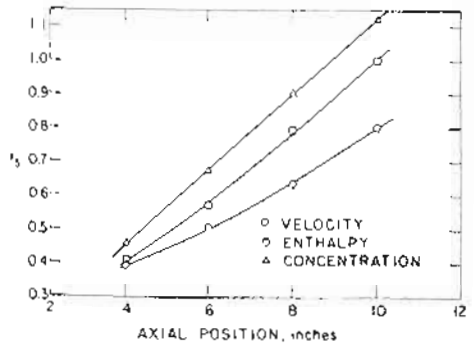

Fig. 10 Jet spreading.

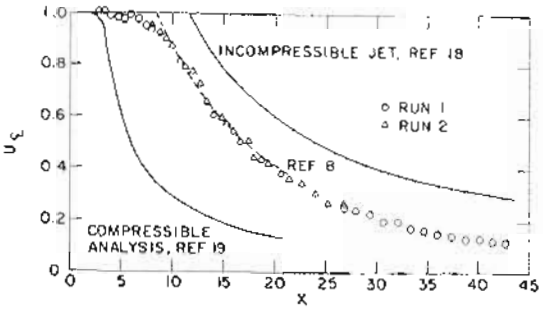

Fig. 11 Velocity distribution-axial-condition 1.

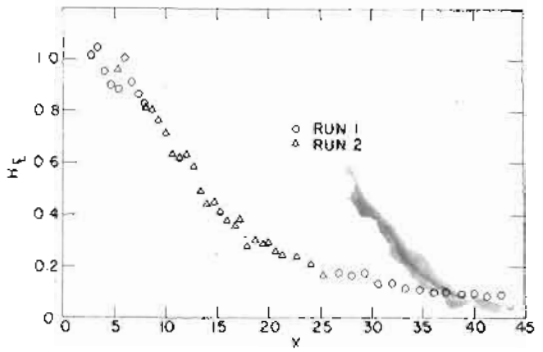

Fig. 12 Stagnation enthalpy distribution-axial-condition 1.

Conclusions

The primary objectives of the investigations were accomplished. A stable high-enthalpy turbulent jet of high subsonic Mach number was successfully probed, and its mixing and decay characteristics thereby established. These results were compared with existing theories and found to agree very well with the prediction of Donaldson and Gray.[8]

The primary conclusions of the present study are listed below.

1) A stable, high-temperature, dissociated jet suitable for investigation of turbulent jet mixing can be produced using electric arc-heater techniques.

2) Mass was found to be transferred more rapidly than energy, which in turn spread more rapidly than did momentum.

3) The high-temperature jets investigated had shorter core lengths and more rapid decay than incompressible jets.

4) The rates of jet spread and decay can be predicted by a theory that properly accounts for the effects of dissociation and the axial variation of the turbulent exchange coefficient as a function of an appropriate Mach number; the magnitude of the basic turbulent mixing mechanism is not affected in a noticeable way by the high enthalpy levels investigated.

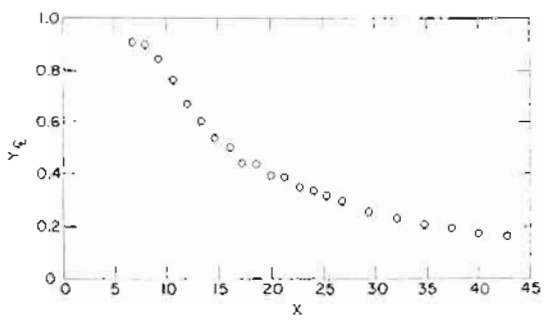

Fig. 13 Concentration distribution-axial-condition 1.